C-CORE Publication No. 91-10

Canadian Acoustics / Acoustique Canadienne 19(3) 17-27 (1991) ***Research article / Article de recherche***

DIRECTIONAL RESPONSE OF A VECTOR INTENSITY HYDROPHONE ARRAY

Jacques Yves Guigné*[1] and Ian Atkinson*

*NORDCO Limited, P.O. Box 8833, St. John's, NF A1B 3T2
[1]C-CORE, Memorial University of Newfoundland, St. John's, NF A1B 3X5

ABSTRACT

This paper describes the test results of a procedure to measure the directional response of a vector intensity hydrophone array. The NORDCO 3-D hydrophone array was designed to simultaneously capture the three components of a sound intensity vector. The phase matched array requires accurate positioning of the receiver elements to achieve a real time response. To calculate the directional response of the array, the x, y and z components of a sound intensity field point produced by a stationary source were measured while rotating the array about its z axis. The resulting sound intensity curves showed the expected cosine patterns with the minima of the x and y components spaced precisely 90° apart.

SOMMAIRE

Cet article décrit les résultats de test d'une méthode afin de mesurer la réponse directionnelle d'une sonde d'intensité vectorielle d'hydrophones. La sonde hydrophonique d'intensité en 3 dimensions, de la compagnie NORDCO a été conçue afin de capturer simultanément les trois composantes du vecteur intensité d'un champ acoustique. La sonde d'intensité aux hydrophones en phase nécessite de positionner avec précision les éléments receveurs afin d'obtenir une réponse en temps réel. Pour calculer la réponse directionnelle de la sonde d'intensité, les composantes vectorelles x, y et z d'un champ acoustique généré par une source stationnaire ont été mesurées en faisant tourner la sonde d'intensité autour de l'axe z. Les courbes d'intensité acoustique ainsi obtenues ont montré que l'on obtenait les variations en cosines espérées avec un écart très précis de 90° entre les minima des composantes en x et en y.

1. INTRODUCTION

The realization of an acoustic wattmeter has been the goal of numerous research scientists. Early work was plagued by instrument and array design errors that were difficult to identify and quantify. T.J. Schultz[1] refers to their work for the U.S. Navy in the early 60's as "a case history in the pathology of over-simplification". Their early results demonstrated and highlighted the importance of understanding the underlying theory and assumptions involved in applying sound intensity measurement techniques.

Researchers persisted despite the early problems encountered. Fahy[2], Hodgson[3], Pavic[4] set the stage for renewed interest in the direct measurement of the sound intensity field. Their papers discuss the theory of using two closely spaced receivers to measure the component of the intensity vector along the direction of the receiver pair (see Appendix). This work was enhanced by Chung[5], Elliott[6], Dyrlund[7] and Shirahatti et al.[8]. They concentrated on the analysis of the errors associated with the measurement of sound intensity. For instance, Chung refers to the phase mismatch error and demonstrates a signal processing technique to eliminate the effect of the phase difference between the two channels. Elliott and Shirahatti et al. discuss the finite difference approximation errors; i.e., the error caused by approximating the pressure gradient by the pressure difference between the two closely spaced receivers. Dyrlund and Seybert[9] address the statistical errors in acoustic intensity measurements. Rasmussen[10,11] illustrates the importance of phase matching and discusses random errors. His work on the effects of a microphone's orientation on the accuracy of the measurement highlights the importance of considering the directionality responses of the individual receivers when designing a sound intensity array.

2. THE 3-D SOUND INTENSITY HYDROPHONE ARRAY

In 1987, NORDCO Limited in association with C-CORE undertook research into sound intensity measurements for underwater geophysical applications in seabed mapping.

By 1988, NORDCO Limited had developed a 3-D sound intensity hydrophone array. Underwater testing and calibration of the array has since taken place.

The hydrophone array consists of three pairs of Bruel & Kjaer omnidirectional hydrophones, phase matched and aligned so that the pairs lie along the mutually orthogonal X, Y and Z axes with the midpoints of the pairs coincident at the geometric center of the array (see Figure 4 for plan view). The spacing between any two paired hydrophones is 5.00 ± 0.01 cm with the measurement made between the geometric centers of the hydrophones. (The geometric center of each hydrophone was assumed to be coincident with its acoustic center). The alignment of the three pairs along the X, Y and Z axes was performed to a similar degree of accuracy. The phased matching procedure was performed with prototype Bruel & Kjaer calibration equipment and standard type 2035 sound intensity analyzers and calibration software. A phase match of better than 50×10^{-3} degrees at 250 Hz exists between any pair of hydrophones.

The objective of this paper is to exhibit the directional response of the array as measured in the reverberant field of a water tank. This is achieved by measuring the X, Y and Z components of intensity emitted from a stationary source while rotating the array about its Z axis.

3. METHODOLOGY

The experiments were performed in the acoustics tank at the Marine Institute of Technology (in Newfoundland). The tank dimensions and physical setup are illustrated in Figure 1. It was recognized that a significant amount of reflected energy would exist in the tank even through the source was pulsed to minimize the accumulation of this energy. This provided a true test for the ability of the sound intensity method to distinguish the active and reactive components of the sound field.

The instrumentation for the experiments is shown in Figure 2. During any one test, two Bruel & Kjaer real-time dual channel, digital filtering analyzers were used. Each analyzer was dedicated to one direction only. With a common clock connection, the analyzers simultaneously measured two components of the intensity vector. (The X and Y directions and the Z and Y directions were normally selected and these plots are shown.) Thus, an intensity vector in the X-Y or Z-Y plane was measured in real time.

The projector was an 8105 hydrophone and this source remained stationary throughout the experiments. The projector transmitted pulses at frequencies of 1, 4, 8 and 10 kHz with various pulse lengths and levels chosen, as indicated, for each experiment. It was necessary to use pulses to minimize the accumulation of reflecting sound waves within the tank from one set-up to the next rotation set-up. A time gating technique was also used to insure that the analysis interval was identical for each rotation measurement location of the array. To ensure proper timing for the measurements, the pulse from the gating unit was also used to trigger the two sound intensity analyzers.

The analyzers were set for 12 mm spacing between transducers. The analyzers were designed for use with microphones in air. The 12 mm space yields an approximate maximum transit time between receivers of 35.8 micro seconds (0.012 metre divided by 335 metres per second). This was the closest setting available for the hydrophone spacing of 50 mm which yields an approximate maximum transit time in water of 33.3 micro seconds (0.050 metres divided by 1500 metres per second). This produces a small error with respect to absolute intensity values but it is constant for each experiment and does not affect the results which only compare relative curve shapes, smoothness and the location of the minima.

Measurements involved 1/2 second linear averaging on the analyzers to ensure that the entire pulse was captured. The collected data were dumped to a computer to free the analyzers for the next measurement at the new rotation point. A printout was generated at the end of each test.

The transmitted signals are illustrated in Figure 3. The function generator produced a sinusoid at the selected frequency for each test. The gating unit truncated the sinusoid with the time window selected creating a pulse which was sent to the power amplifier and the projector. This window was also sent from the gating unit to a trigger box which controlled both sound intensity analyzers (see Figure 2).

The pulse length was normally set at 250 milliseconds. The pulse levels, controlled by the power amplifier, were varied depending on the desired frequency of the source. This was necessary since the 8105 hydrophone which was used as a projector is not an efficient transmitter at these low frequencies. Thus, its output level at 1 kHz is very much lower than at 8 kHz if the input level is held constant. Even with the changes in output levels, noted below, the difference between the measured intensity levels at different frequencies is clearly evident from the plots.

A further note on the pulse length must be made. For a 250 millisecond pulse in a small water tank, it is clear that numerous reflections occur and are incident upon the hydrophone array during the analysis window. It is a characteristic of the sound intensity technique that the array discriminated between the active component of the sound

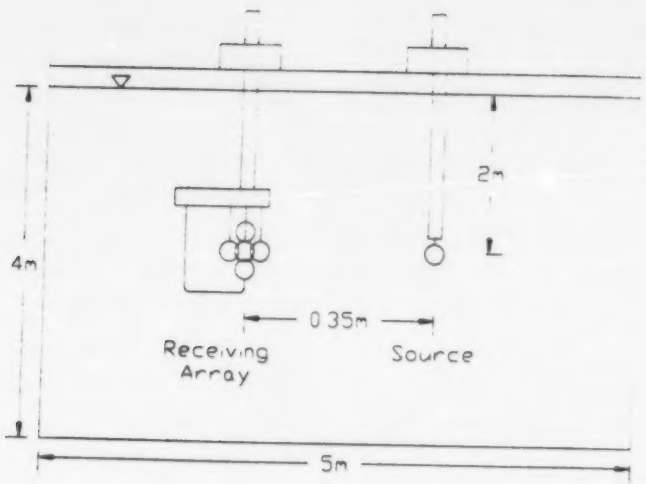

FIGURE 1 Physical setup. Note tank width is 4m.

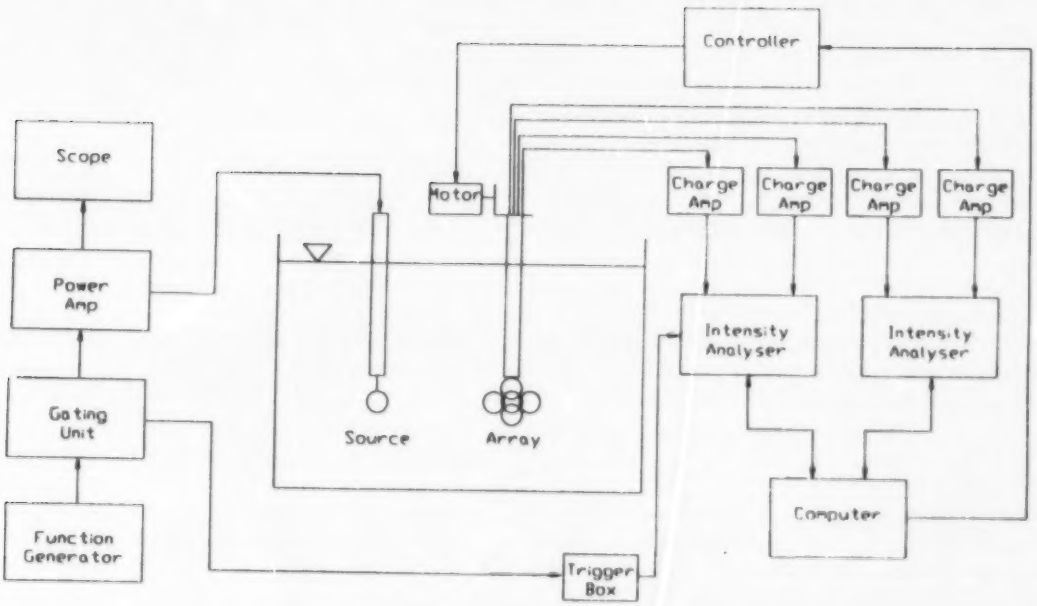

FIGURE 2 Instrumentation

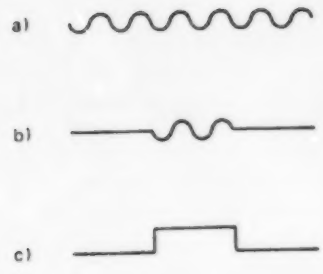

FIGURE 3 Signal waveforms, a) from function generator
b) from gating unit to source.
c) from gating unit to analysers.

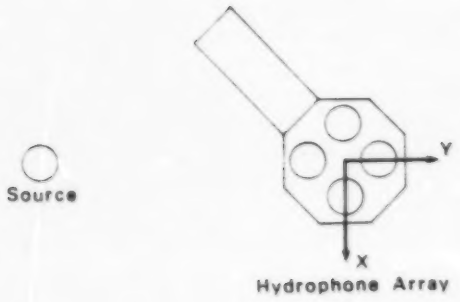

FIGURE 4 Initial (0 degree) position of array showing X and Y directions.

field produced by the source and the background reverberations.

To determine the directional response of the hydrophone array, the array was rotated counter-clockwise about its Z axis while measurements were made at incremental steps. The initial (0°) position of the array is shown in Figure 4. The X and Y directions are also delineated in this figure. After each test, the array was rotated clockwise back to its 0° position. Rotation of the array was controlled by the computer and confirmed by visually checking a scale inscribed on the turntable.

The data are plotted as directional characteristics curves using polar coordinates, as shown in Figure 5 to 14.

4. RESULTS AND INTERPRETATION

The array was set to the zero position by visual inspection and rotated 360° with an X-Y measurement recorded at each 1° increment. The source was set to produce a 250 ms pulse at 8 kHz with a signal generator output of 10 mV. The measurement was performed three times generating three nearly identical curves of the array response at 8 kHz. Figure 5 displays one of these response curves.

The curve shows the expected cosine patterns with minima spaced precisely 90° apart. The 10° offset from the zero position is due to a slight misalignment between the array and turntable axes arising from the dependence on visual inspection for the initial positioning of the array. This 10° offset was eliminated by resetting the zero position for all subsequent experiments.

The analyzers were also set to record sound pressure rather than intensity in the X-Y plane. Two 360° rotations were required. During the first, the channel A pressure on both analyzers (hydrophones A and B in Figure 6a) was measured, and during the second, both channel B pressures (hydrophones C and D in Figure 6b) were measured. Ambient reverberation now becomes an obvious problem when measuring only pressure since both the reactive and active components of the field are captured and summed. This is evident from the jagged appearance of the pressure data curves. For this dataset the pressure measured by an individual hydrophone in the array for each new rotated location is different due to the spatial variation of the sound field created by the interaction of the reflected energy which varies from point to point. The sound intensity dataset produces smooth curves since the intensity measurement is taken at a single point at the center of the array for all array orientations. Thus, the background reverberations at this point are constant for every measurement position.

The array was again set to the zero position and rotated 360° with the source producing a 250 ms pulse at 4 kHz with a signal generator output of 15 mV. The plot of Figure 7 exhibits the intensity array response at 4 kHz for 1° incremental steps. As in the 8 kHz plot (Figure 5), the expected curves were generated with minima separated by 90°.

The source was then set to produce a 250 ms pulse at 1 kHz with a level of 120 mV. Figure 8 resembles the cosine bell curves although the plots are slightly skewed as minima are not precisely 90° apart. Some roughness (not evident in the drafted figure) in the cosine curves exists. The roughness of the curves can be explained by sporadic incoherence in the transmission signal due to the low frequency of propagation which is outside of the normal operational frequencies of the projector. This interference, which did not exist at higher frequencies, was evident in the analysis during the testing.

After locating a minima at 80° (Figure 5), the array was rotated counterclockwise 60° from the initial position. The test began here as the array was rotated a further 36° with measurements taken at every 0.1° increments. This test was performed to observe the detail of the array response about the null point. Figure 9 was generated with the source set to produce a 250 ms pulse at 8 kHz with a level of 12 mV. The noise in the curves is interesting and could be related to the physical interference of the hydrophone elements with the passing sound wave. This interference phenomenon is consistent on both X and Y components. It is important to note the symmetry about the null point of the Y component. It is only evident when rotations of 0.1 degree are implemented indicating that we are observing "resonant like" internal reflection effects within the array. The coarser 1° sampling smooths over this fine structure of the array response. Further investigation of this phenomenon is warranted.

The Z pair of hydrophones was then connected to the second analyzer to allow the measurement of the Y and Z components of intensity. The source was set to produce a 250 ms, 8 kHz pulse at 15 mV. A plot was generated for the 6.3 kHz pulse at 15 mV (Figure 10).

In this figure the Z direction plot is low and an almost perfect circle is expected since the Z components should be constant and at a minimum. The fact that the curve is not exactly at a minimum is a result of the source and acoustic center of the array being at slightly different depths. Slight imperfections in the circle are due to the array not hanging exactly vertically in the tank. The skewed circle is therefore produced. The supporting bracket was visually set and plumbed and slight errors in the alignment were noted. The plot is, however, close to the expected behavioural shape.

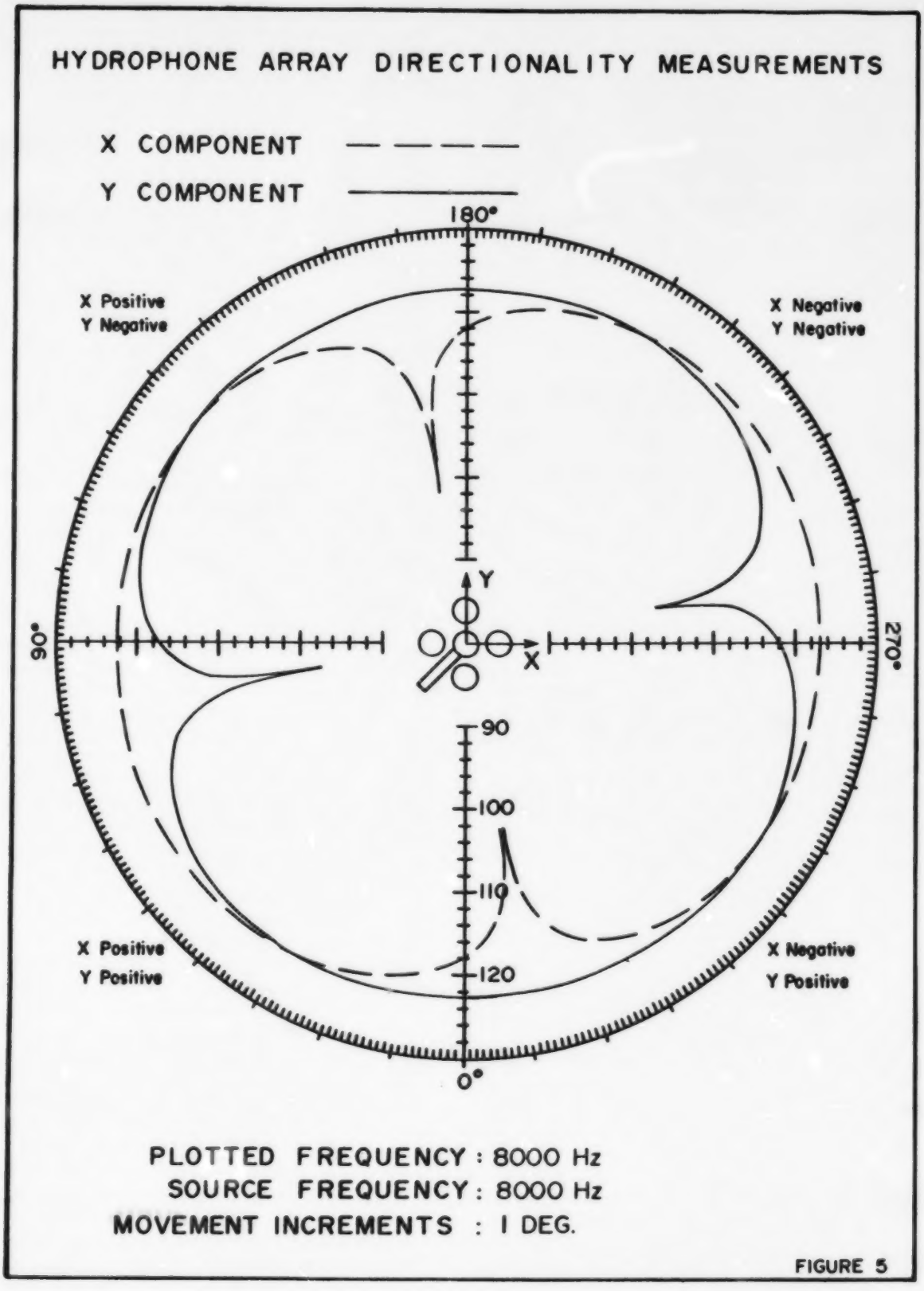
HYDROPHONE ARRAY DIRECTIONALITY MEASUREMENTS
X COMPONENT
Y COMPONENT
180°
X Positive
Y Negative
X Negative
Y Negative
90°
270°
Y
X
90
100
110
120
X Positive
Y Positive
X Negative
Y Positive
0°
PLOTTED FREQUENCY : 8000 Hz
SOURCE FREQUENCY : 8000 Hz
MOVEMENT INCREMENTS : 1 DEG.

FIGURE 5

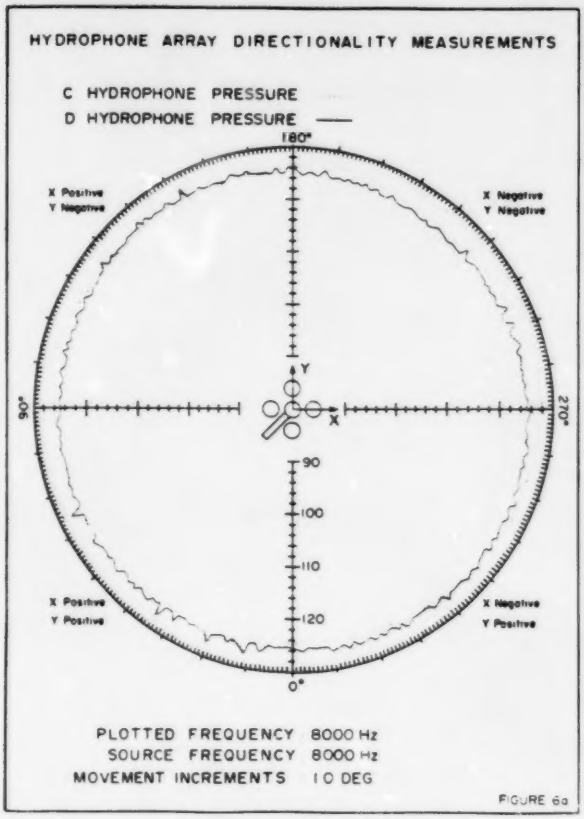
HYDROPHONE ARRAY DIRECTIONALITY MEASUREMENTS
C HYDROPHONE PRESSURE
D HYDROPHONE PRESSURE
180°
X Positive Y Negative
X Negative Y Negative
90°
270°
Y
X
90
100
110
120
X Positive Y Positive
X Negative Y Positive
0°
PLOTTED FREQUENCY 8000 Hz
SOURCE FREQUENCY 8000 Hz
MOVEMENT INCREMENTS 1.0 DEG
FIGURE 6a

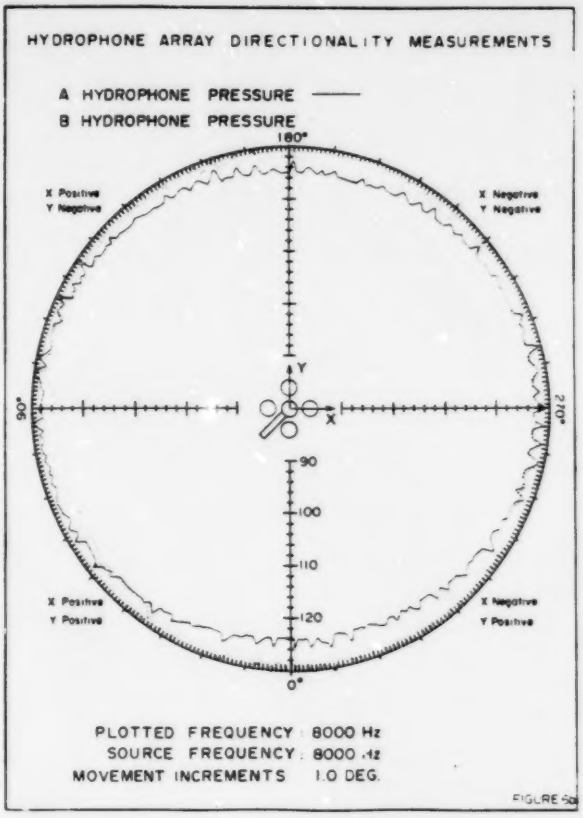
HYDROPHONE ARRAY DIRECTIONALITY MEASUREMENTS
A HYDROPHONE PRESSURE
B HYDROPHONE PRESSURE
180°
X Positive Y Negative
X Negative Y Negative
90°
270°
Y
X
90
100
110
120
X Positive Y Positive
X Negative Y Positive
0°
PLOTTED FREQUENCY 8000 Hz
SOURCE FREQUENCY 8000 Hz
MOVEMENT INCREMENTS 1.0 DEG.
FIGURE 6b

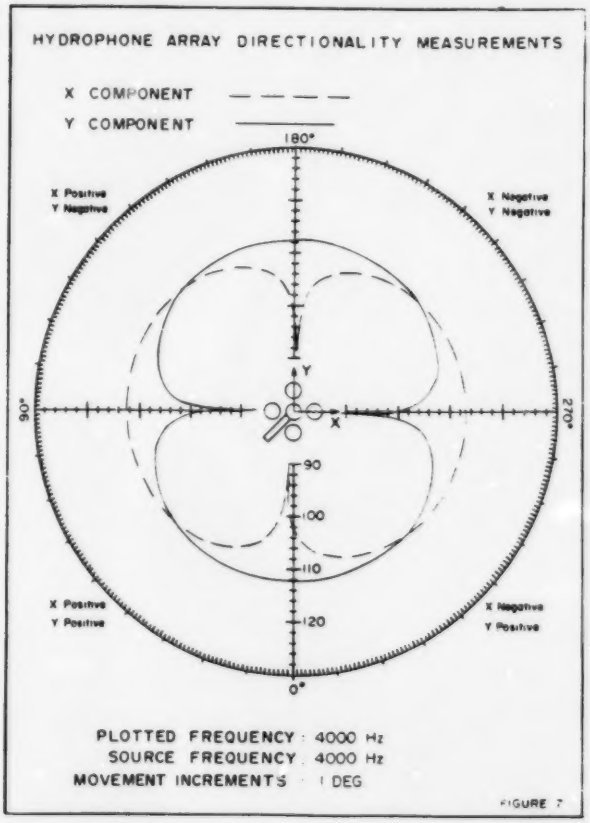
HYDROPHONE ARRAY DIRECTIONALITY MEASUREMENTS
X COMPONENT
Y COMPONENT
180°
X Positive Y Negative
X Negative Y Negative
90°
270°
Y
X
90
100
110
120
X Positive Y Positive
X Negative Y Positive
0°
PLOTTED FREQUENCY 4000 Hz
SOURCE FREQUENCY 4000 Hz
MOVEMENT INCREMENTS 1 DEG
FIGURE 7

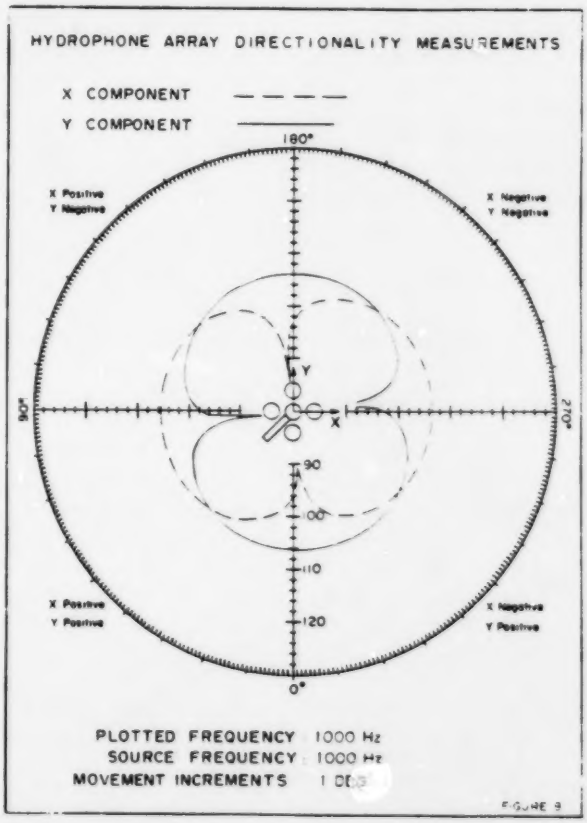
HYDROPHONE ARRAY DIRECTIONALITY MEASUREMENTS
X COMPONENT
Y COMPONENT
180°
X Positive Y Negative
X Negative Y Negative
90°
270°
Y
X
90
110
120
X Positive Y Positive
X Negative Y Positive
0°
PLOTTED FREQUENCY 1000 Hz
SOURCE FREQUENCY 1000 Hz
MOVEMENT INCREMENTS 1 DEG
FIGURE 9

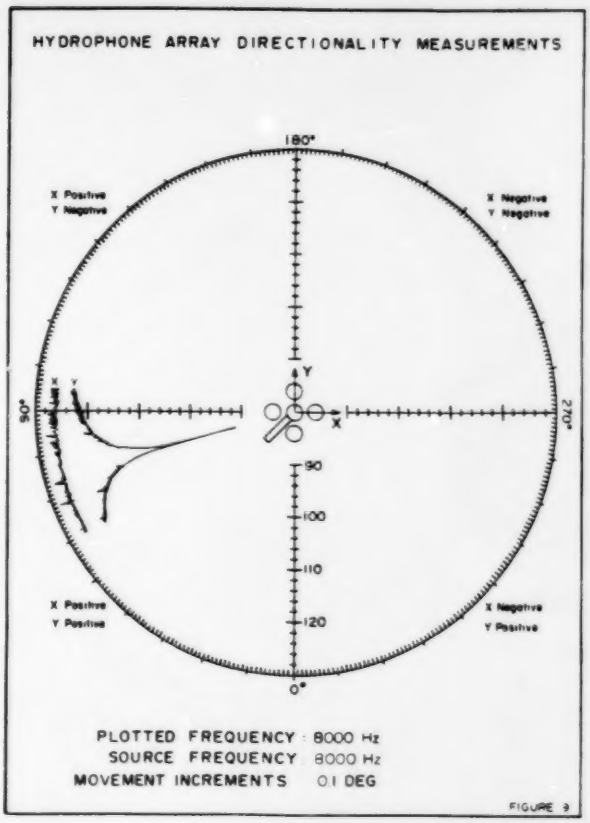

FIGURE 9

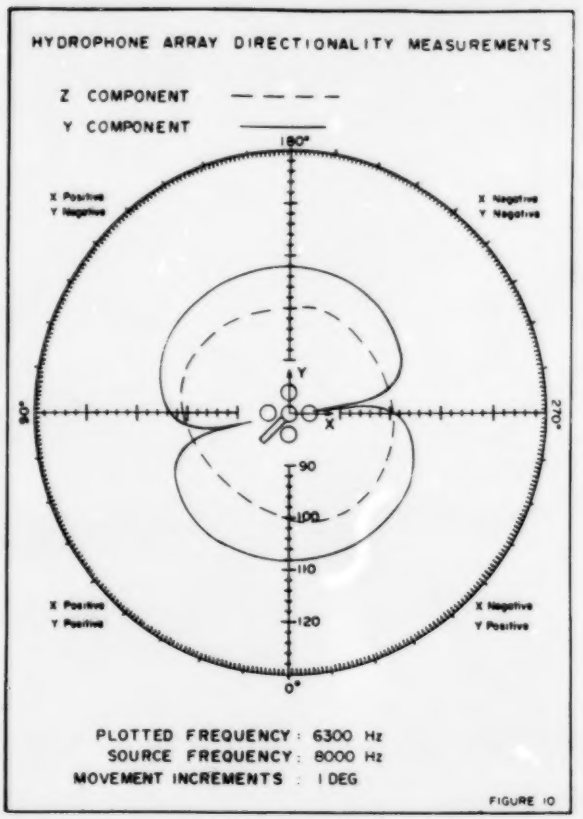

FIGURE 10

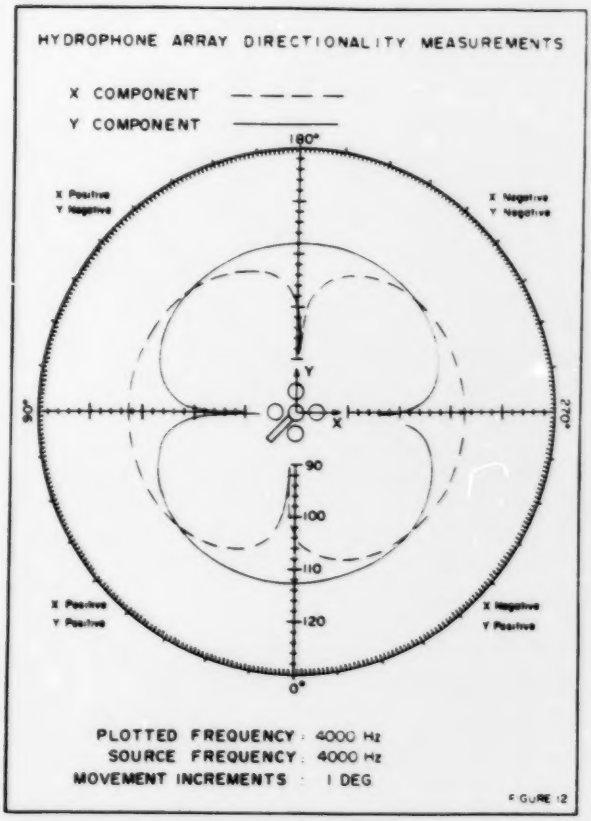

FIGURE 12

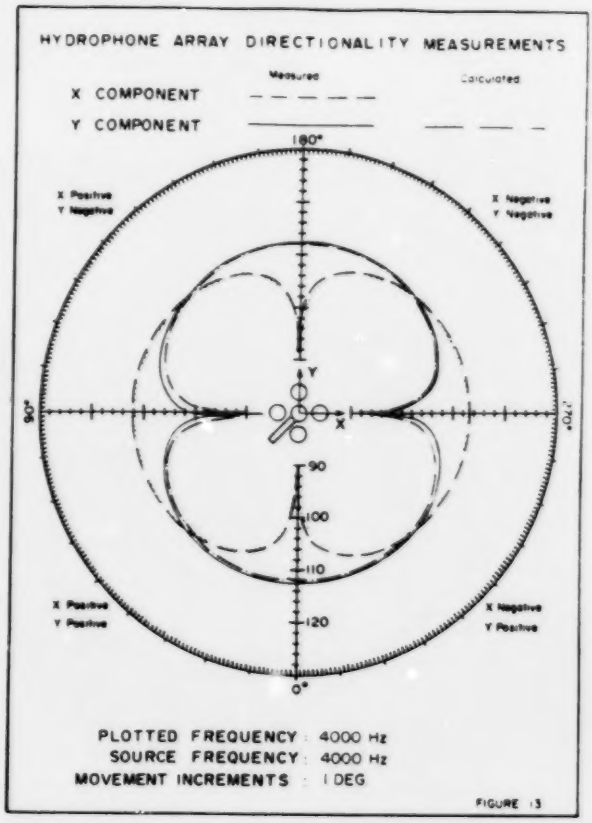

FIGURE 13

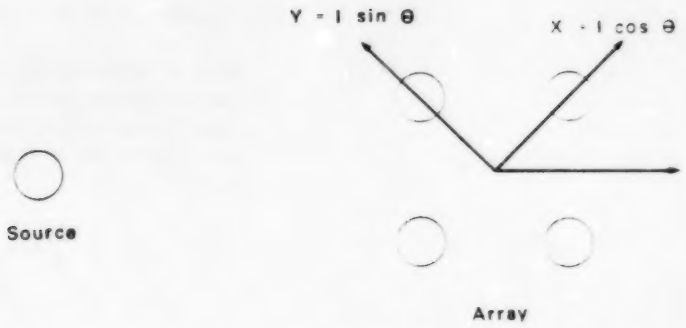

FIGURE 11 Intensity vector components

NORDCO Robotic ASI
3-D Sound Intensity Hydrophone Array
(Preliminary Design Nov. 1987)

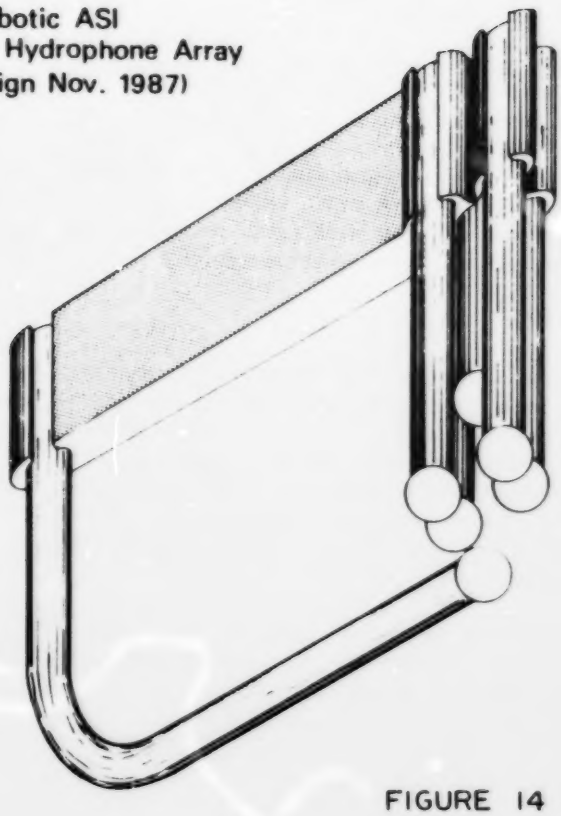

FIGURE 14

Theoretical curves were computed for the X-Y tests at 4 kHz for comparison to the corresponding experimental curves. An example of the measured 4 kHz plot is shown in Figure 12 whilst Figure 13 illustrates the same data against theoretical curves. The calculations used the following relationships:

$$X = I \cos \theta$$
$$Y = I \sin \theta$$

where θ is the rotation of the array from the initial position (see Figure 11) and I is the maximum intensity value measured which represents the magnitude of the source intensity vector.

5. CONCLUSION

The NORDCO underwater 3-D vector intensity array has a directionality response that closely matches the ideal, theoretical response. This provides confidence that the array is performing correctly allowing true sound intensity data to be acquired underwater. It should be noted that the data was acquired in a reverberant sound field. Clearly, the ability of the sound intensity method to accurately measure the source amplitude and direction in this type of field demonstrates its superiority over conventional pressure receivers.

The advantages of the vector intensity approach are in its signal-to-noise ratio, 1° directivity at low frequencies (e.g. 1 kHz), incoherent noise suppression, and sound intensity mapping of dominant energy paths. Future work will be on beamforming with this intensity array. Simple algorithms can be applied using the approach to identify sound patterns in the water such as for automatic event detection and for spatial, temporal and spectral signal decomposition.

APPENDIX

The technique of directly measuring the vector component of sound intensity along the axis of two closely spaced receivers requires careful phase matching of the receiver pair. The spacing between the receivers is optimized for the desired measurement frequency range. The directionality plots of the individual receiver elements is also an important consideration. Each element should ideally be omnidirectional.

The measurement technique relies on the pressure difference between the two receivers to provide an estimate of the pressure gradient at center of the array.

$$\nabla p = \frac{p_1 - p_2}{\Delta r}$$

where Δr is the spacing between receiver 1 and 2.

Integrating the pressure gradient over time gives an estimate of the particle velocity provided that there is zero mean flow of the fluid through which the sound wave is propagating. The derivation of this is from Euler's equation for fluid momentum.

$$\rho \frac{\partial v_r}{\partial t} + \frac{\partial p}{\partial r} = 0$$

where ρ is the fluid mass density. Therefore

$$v_r = \frac{1}{\rho \Delta r} \int_o^t (p_1 - p_2)\, dt$$

Since the component of the vector intensity along the receiver pair axis, I_r, can be given by the time average of the product of the acoustic pressure and the particle velocity at a point,

$$I_r = \langle p(t).v_r(t) \rangle$$
$$= \left\langle \frac{p_1 + p_2}{2} \cdot \frac{1}{\rho \Delta r} \int_o^t (p_1 - p_2)\, dt \right\rangle$$

The importance of phase matching the array is thus obvious.

To measure the three components of the sound intensity vector at a point it is necessary to orient three pairs of receivers along the three orthogonal axes, X, Y and Z so that the center point of each pair is coincident.

Since the original tests were performed in 1988 with the Bruel & Kjaer sound intensity analyzers, electronic receiver boards and controllers have been developed at NORDCO Limited to permit the measurement of sound intensity in the underwater environment using the FFT method.

ACKNOWLEDGEMENTS

The authors wish to acknowledge the support of Mr. Gareth Williams in the data collection and Mr. Gunnar Rasmussen of Bruel & Kjaer Ltd. for his advice.

REFERENCES

1. Schultz, T.J., Smith, P.W. and Malme, C.I. (1975). "Measurement of Acoustic Intensity in a Reactive Sound Field", J. Acoust. Soc. Am., Vol. 57, No. 6, Part I, June 1975.

2. Fahy, Frank J. (1977). "Measurement of Acoustic Intensity Using the Cross-spectral Density of Two Microphone Signals", J. Acoust. Soc. Am., Vol. 62, No. 4, October 1977.

3. Hodgson, T.H. (1977). "Investigation of the Surface Acoustical Intensity Method for Determining the Noise Sound Power of a Large Machine in situ", J. Acoust. Soc. Am., Vol. 61, pp. 487-493.

4. Pavic, G. (1977). "Measurement of Sound Intensity", Journal of Sound and Vibration, Vol. 51, No. 4, pp. 533-545.

5. Chung, J.Y. (1978). "Cross-spectral Method of Measuring Acoustic Intensity Without Error Caused by Instrument Phase Mismatch", J. Acoust. Soc. Am., Vol. 64, No. 6, December 1978.

6. Elliott, S.J. (1981). "Errors in Acoustic Intensity Measurements", Letters to the Editor, Journal of Sound and Vibration, Vol. 78, Vol. 3, 1981.

7. Dyrlund, D. (1983). "A Note on Statistical Errors in Acoustic Intensity Measurements", Letters to the Editor, Journal of Sound and Vibration, Vol. 90, No. 4, 1983.

8. Shirahatti, U.S., Crocker, M.J. and Raju, P.K. (1988). "Finite Difference Approximation Errors in Sound Intensity Estimates of Interfering Sources", J. Acoust. Soc. Am., Vol. 84, No. 2, August 1988.

9. Seybert, A.F. (1981). "Statistical Errors in Acoustic Intensity Measurements", Journal of Sound and Vibration, Vol. 75, 1981.

10. Rasmussen, P. (1985). "Phase Errors in Intensity Measurements", Bruel & Kjaer, Dept. 13: Intensity Measurements, January 1985.

11. Rasmussen, P. (1985). "Random Error in Sound Power Measurement Using Sound Intensity", Bruel & Kjaer, Dept. 13: Intensity Measurements, January 1985.